

# Optimised control of Stark-shift-chirped rapid-adiabatic-passage in a $\Lambda$ -type three-level system

Johann-Heinrich Schönfeldt,\* Jason Twamley, and Stojan Rebić  
Centre for Quantum Computer Technology, Physics Department,  
Macquarie University, Sydney, NSW 2109, Australia

Inhomogeneous broadening of energy levels is one of the principal limiting factors for achieving “slow” or “stationary” light in solid state media by means of electromagnetically induced transparency (EIT), a quantum version of stimulated Raman adiabatic passage (STIRAP). Stark-shift-chirped rapid-adiabatic-passage (SCRAP) has been shown to be far less sensitive to inhomogeneous broadening than STIRAP, a population transfer technique to which it is closely related. We further optimise the pulses used in SCRAP to be even less sensitive to inhomogeneous broadening in a  $\Lambda$ -type three-level system. The optimised pulses perform at a higher fidelity than the standard gaussian pulses for a wide range of detunings (i.e. large inhomogeneous broadening).

PACS numbers: 32.80.Qk, 33.20.Bx, 33.80.Be, 42.50.Hz, 42.50.Gy

## I. INTRODUCTION

Atomic vapours have been extensively investigated for use as quantum information storage media by “slowing down”, or even “stopping”, a light pulse carrying quantum information. This is achieved by mapping the quantum state of the light to a long-lived spin state in an ensemble of atoms by means of a reversible process: electromagnetically induced transparency (EIT) [1, 2, 3, 4, 5], which is closely related to an adiabatic passage technique known as Stimulated Raman Adiabatic Passage (STIRAP). The homogeneity of the atomic vapour atoms means that the light pulses used in EIT experiments in these systems can be tuned to specific transitions in the atoms and that these light fields will then interact strongly with all the atoms in the ensemble.

Solid-state implementations of stored light by means of EIT may have a number of potential advantages over atomic vapour implementations. They have potential to greatly reduce (possibly eliminate) limitations on the storage lifetime, which is mainly due to atomic diffusion and Doppler velocities in atomic vapour systems. A higher atomic density has the potential to yield a stronger interaction between the light and atomic ensemble, whilst being more compact and simple to use/manufacture may indicate great scalability [6] on the part of solid-state implementations. EIT and slow light have been demonstrated in rare-earth doped semiconductors e.g. *Pr* doped  $Y_2SiO_5$  [7, 8], whereas only EIT has thus far been shown in nitrogen-vacancy colour centers in diamond [9, 10]. Solid-state media are, however, not without their own problems, the biggest of which is inhomogeneous broadening of the energy levels, which leads to

a reduction in the number of atoms/centers that will be resonant with the incident optical field. This broadening occurs because each atom/center experiences a different electronic environment due to a number of factors e.g. the local strains in the crystal lattice.

Recently a variation of STIRAP (the basis of EIT), namely Stark-shift-chirped rapid adiabatic passage (SCRAP), has been shown to perform coherent population transfer with a high fidelity for a range of different detunings in a  $\Lambda$ -type three-level system [11]. That is, SCRAP is far more robust when there is large inhomogeneous broadenings present in the ensemble. In SCRAP, a separate (pulsed) field is added to the STIRAP fields to induce Stark shifts in the energy levels and thus bring the required, initially off-resonant, transitions on resonance at specific times. We propose that a quantum version of SCRAP could surmount some of the limitations that inhomogeneous broadening places on “slow” light in solid state systems. We will examine this further in future work.

In this work we make use of optimum control techniques similar to Khaneja *et al.* (2005) [12], in order to optimise the standard SCRAP pulses so as to minimise the decrease in fidelity brought on by inhomogeneous broadenings of the transitions. To measure this we simulate the SCRAP process population transfer between two long lived ground states which experience large detunings due to inhomogeneous broadening. Our main result is that we can improve the average fidelity of population transfer over a wide range of detunings for both the ground to excited state detuning and the ground to target state detuning (two-photon detuning). The optimal control pulses are thus tailored to provide effective state transfer (and thus EIT), in the presence of large inhomogeneous broadening.

The paper is arranged as follows: In section II the SCRAP technique is introduced. Section III describes the optimisation methods used. Section IV shows the results for the optimised pulses. Conclusions are drawn in Section V.

---

\*E-mail: jhschonf@ics.mq.edu.au

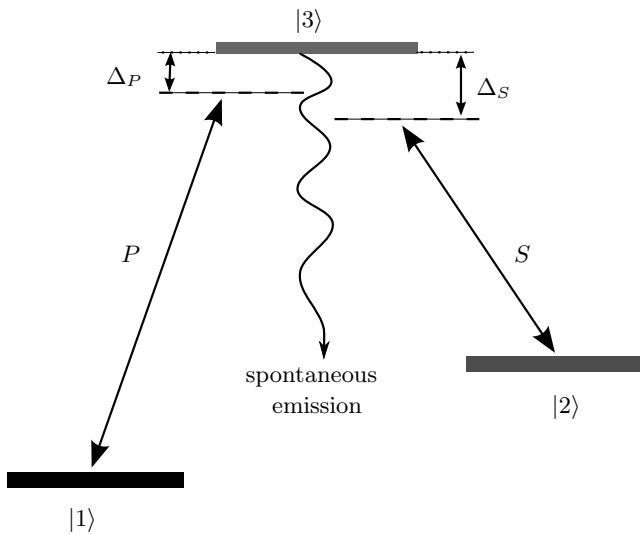


FIG. 1: The  $\Lambda$ -type three-level energy scheme. States  $|1\rangle$  and  $|2\rangle$  are coupled by the pump pulse  $P$  which has a detuning  $\Delta_P$  from being exactly on resonance. Similarly states  $|2\rangle$  and  $|3\rangle$  are coupled by the Stokes pulse  $S$  which has a detuning  $\Delta_S$ . State  $|2\rangle$  is short lived with spontaneous emission occurring out of the system.

## II. SCRAP

The Stark-chirped rapid adiabatic passage technique (SCRAP) was first proposed by Yatsenko *et al.* [13], and implemented by Rickes *et al.* [14], in two-level systems as an efficient method for complete population transfer between two states. It was later shown by Rangelov *et al.* (2005) [11], that a Stark shifting pulse can also be used to achieve complete population transfer through adiabatic passage in a three-level system, thus providing an alternative to STIRAP.

The  $\Lambda$ -type three-level system (Figure 1), is comprised of two long lived ground states, one the initially populated state ( $|1\rangle$ ), and the other the target state ( $|3\rangle$ ), and an excited state ( $|2\rangle$ ). In general the excited state has a short life time: STIRAP is effective at complete population transfer since it avoids populating the excited state by having the system evolve along a dark-state. In both SCRAP and STIRAP states  $|1\rangle$  and  $|2\rangle$  are coupled by the ‘‘pump’’ laser pulse whilst states  $|3\rangle$  and  $|2\rangle$  are coupled by the ‘‘Stokes’’ laser pulse. The frequencies of these two classical laser fields are typically not exactly on resonance with their respective transitions, and have detunings  $\Delta_P$  and  $\Delta_S$  for the pump and Stokes lasers respectively. Herein lies the advantage that SCRAP has over STIRAP: STIRAP requires exact two-photon resonance ( $\Delta_P - \Delta_S = 0$ ) in order to be effective, whereas SCRAP has a larger tolerance for two-photon detuning. In SCRAP a third strong far-off-resonance laser pulse, the Stark pulse, is also applied. The Stark pulse induces a Stark shift in the energy of the excited state (essen-

tially leaving the energy of the lower levels unchanged), thus bringing the initially off-resonant transitions into resonance. The Stark shift causes the diabatic energy of state  $|2\rangle$  to cross those of states  $|1\rangle$  and  $|3\rangle$ , allowing population transfer from  $|1\rangle$  to  $|2\rangle$  and then to  $|3\rangle$ , completing the population transfer. It is thus clear that the diabatic energies of state  $|1\rangle$  and  $|2\rangle$  must cross before the crossing of energies of states  $|2\rangle$  and  $|3\rangle$ . It is also clear that decay out of the excited state will play a role in SCRAP, as opposed to STIRAP.

In the rotating wave approximation, the Hamiltonian of the  $\Lambda$ -type three-state system depicted in Figure 1 is

$$H(t) = \frac{\hbar}{2} \begin{bmatrix} 0 & \Omega_P(t) & 0 \\ \Omega_P(t) & 2(\Delta_P + S_2(t)) - i\Gamma & \Omega_S(t) \\ 0 & \Omega_S(t) & 2(\Delta_P - \Delta_S) \end{bmatrix}, \quad (1)$$

where  $\Omega_P(t)$  and  $\Omega_S(t)$  are respectively the pump and Stokes laser field Rabi frequencies and  $S_2(t)$  is the Stark shift in the energy of the excited energy level  $|2\rangle$  due to a third far-off-resonant laser pulse (Stark pulse). For the examples here it is assumed that the Stark shift is negative,  $S_2(t) < 0$ . The detunings of the pump and Stokes fields are  $\Delta_P$  and  $\Delta_S$  respectively. The imaginary term  $i\Gamma$  describes the losses from  $|2\rangle$  due to spontaneous radiative decay out of the three-level system. The Stark shifts of the energy levels for states  $|1\rangle$  and  $|3\rangle$  are not included here because Stark shifts in ground and metastable states tend to be much smaller than those of excited states.

In Rangelov *et al.* (2005) [11]), gaussian pulse shapes were used for all the pulses, with identical peak values,  $\Omega_0$ , for the Rabi frequencies of the pump and Stokes pulses,

$$\Omega_p(t) = \Omega_0 e^{-(t-\tau_p)^2/T_p^2}, \quad (2)$$

$$\Omega_s(t) = \Omega_0 e^{-(t-\tau_s)^2/T_s^2}, \quad (3)$$

$$-S_2(t) = S(t) = S_0 e^{-t^2/T_{St}^2}. \quad (4)$$

The peak of the Stark pulse (maximum Stark shift of  $S_0$ ) is taken to be at  $t = 0$ , and as such the pump and Stokes pulses peak at times  $\tau_p$  and  $\tau_s$  respectively. The pulse durations are determined by  $T_P$ ,  $T_S$  and  $T_{St}$ , where it was taken that the pump and Stokes pulses have equal duration  $T_P = T_S$  and the Stark pulse has twice their duration  $T_{St} = 2T_P$ . The unit of time was defined as  $T_P$  and the unit of frequency as  $1/T_P$ . These gaussian pulses served as exemplars for the initial pulses used in our optimising routine, see section III.

The diabatic energies of the states are

$$E_{|1\rangle} = 0, \quad (5)$$

$$E_{|2\rangle} = 2(\Delta_P + S_2(t)), \quad (6)$$

$$E_{|3\rangle} = 2(\Delta_P - \Delta_S), \quad (7)$$

which with the condition that the Stark shift is negative ( $S_2(t) < 0$ ), dictates that the diabatic energy of state  $|2\rangle$ ,  $E_{|2\rangle}$ , will only cross those of states  $|1\rangle$  and  $|3\rangle$  when

$$S_0 > \Delta_P > 0, \quad (8)$$

and

$$S_0 > \Delta_S > 0. \quad (9)$$

With the condition that the Stark shift is negative two distinct situations can arise: the two-photon detuning can be negative

$$\Delta_P > 0 > (\Delta_P - \Delta_S) > \Delta_P - S_0, \quad (10)$$

or positive

$$\Delta_P > (\Delta_P - \Delta_S) > 0 > \Delta_P - S_0. \quad (11)$$

In the examples used here to explain the SCRAP technique, and for the pulse optimisation, only the first case (10), where the two-photon detuning is negative will be presented ( $\Delta_P < \Delta_S$ ). In the case that the two-photon detuning is positive (11), the order of the pulses in standard SCRAP must be run in reverse to what will be shown here, [11].

Our goal is to achieve efficient state transfer for as wide a variety of detunings as possible, for which SCRAP is the ideal technique. The population transfer for the ideal situation with no detuning, no decay, and using pulse parameters out of [11] is shown in Figure 2. In such a situation with no detuning STIRAP would be the preferred technique. For a more detailed explanation of three state SCRAP please refer to section III in Rangelov *et al.* (2005) [11].

### III. OPTIMISATION THROUGH OPTIMAL CONTROL

The above mentioned SCRAP process has the advantage that it can tolerate large two-photon detunings, but unlike STIRAP it suffers from decay from state  $|2\rangle$ . In this section we will use an optimisation technique, based on the GRAPE algorithm by Khaneja *et al.* (2005) [12], to optimise the transfer fidelity for a set of detunings. The state of the three level system is characterised by the density operator  $\rho(t)$  with the Liouville-von Neuman equation of motion

$$\dot{\rho}(t) = -i \left[ \left( H_0 + \sum_{k=1}^m u_k(t) H_k \right), \rho(t) \right]. \quad (12)$$

Where  $H_0$  is the free evolution Hamiltonian and the  $H_k$  are the Hamiltonians corresponding to the  $m$  control fields (the Stokes, pump and Stark fields).  $u(t) =$

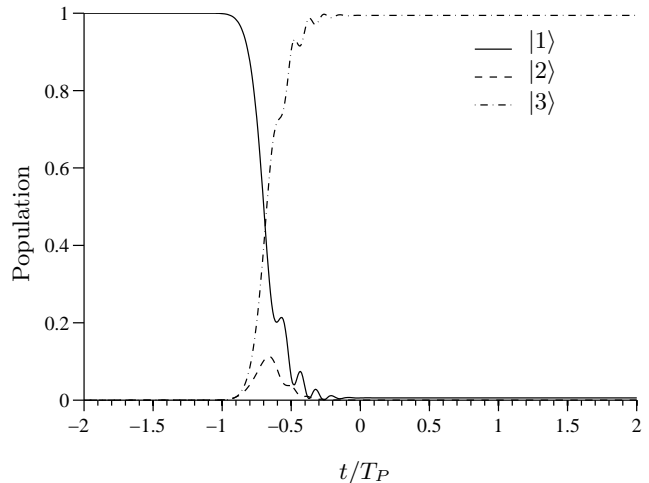


FIG. 2: The evolution of the population in the 3-state-system (state  $|1\rangle$  solid line,  $|2\rangle$  dashed line and  $|3\rangle$  dash-dotted line) where the pulses used were the original gaussians with the following parameters:  $\Delta_P = 30/T_P$ ,  $\Delta_S = 45/T_P$ ,  $S_0 = 200/T_P$ ,  $\Omega_0 = 50/T_P$ ,  $T_S = T_P$ ,  $T_{St} = 2T_P$ ,  $\tau_p = -T_P$ ,  $\tau_s = -2T_P$ . There was no decay out of state  $|2\rangle$ , ( $\Gamma = 0$ ).

( $u_1(t), u_2(t), \dots, u_m(t)$ ) is the vector of control amplitudes. We discretised the transfer time  $T$  into  $N$  steps of length  $\Delta t = T/N$ , and assume that the amplitude for each control field is constant during each time step. Instead of optimising these amplitudes directly, as described in [12], we define each amplitude vector in terms of  $q$  gaussians,

$$u_k(j) = \sum_{n=1}^q h_{n,k} \exp \left[ - (j\Delta t - \tau_{n,k})^2 / \sigma_{n,k}^2 \right], \quad (13)$$

that sum to create the pulse for the specific control field, and optimise the parameters of these gaussians. The aim is to find the parameters ( $h_{n,k}, \tau_{n,k}, \sigma_{n,k}$ ) that will, given the initial density operator  $\rho(0) = \rho_0$ , maximise the overlap of the density operator after a time  $T$ ,  $\rho(T)$ , with a target density operator  $C$ . The overlap is measured by the standard inner product, thus the performance index  $\Phi_0$  is given by

$$\Phi_0 = \langle C | \rho(t) \rangle. \quad (14)$$

During each time step  $j$  the evolution of the system is given by the propagator

$$U_j = \exp \left[ -i\Delta t \left( H_0 + \sum_{k=1}^m u_k(j) H_k \right) \right]. \quad (15)$$

The performance index can then be written as

$$\Phi_0 = \underbrace{\langle U_{j+1}^\dagger \dots U_N^\dagger C U_N \dots U_{j+1} \rangle}_{\lambda_j} \underbrace{\langle U_j \dots U_1 \rho_0 U_1^\dagger \dots U_j^\dagger \rangle}_{\rho_j}. \quad (16)$$

From [12] we have that

$$\frac{\delta\Phi_0}{\delta u_k(j)} = -\langle \lambda_j | i\Delta t [H_k, \rho_j] \rangle, \quad (17)$$

but we are interested in the gradient with regard to  $h_{n,k}$ ,  $\tau_{n,k}$  and  $\sigma_{n,k}$ :

$$\begin{aligned} \frac{\delta\Phi_0}{\delta h_{n,k}} &= \sum_j^N \left[ \frac{\delta\Phi_0}{\delta u_k(j)} \times \frac{\delta u_k(j)}{\delta h_{n,k}} \right] \\ &= \sum_j^N -\langle \lambda_j | i\Delta t [H_k, \rho_j] \rangle \times \\ &\quad \exp \left[ -(j\Delta t - \tau_{n,k})^2 / \sigma_{n,k}^2 \right], \end{aligned} \quad (18)$$

and similarly

$$\frac{\delta\Phi_0}{\delta \tau_{n,k}} = \sum_j^N -\langle \lambda_j | i\Delta t [H_k, \rho_j] \rangle \times \frac{2(j\Delta t - \tau_{n,k})}{\sigma_{n,k}^2} \times h_{n,k} \exp \left[ -(j\Delta t - \tau_{n,k})^2 / \sigma_{n,k}^2 \right], \quad (19)$$

$$\frac{\delta\Phi_0}{\delta \sigma_{n,k}} = \sum_j^N -\langle \lambda_j | i\Delta t [H_k, \rho_j] \rangle \times \frac{2(j\Delta t - \tau_{n,k})^2}{\sigma_{n,k}^3} \times h_{n,k} \exp \left[ -(j\Delta t - \tau_{n,k})^2 / \sigma_{n,k}^2 \right]. \quad (20)$$

The performance  $\Phi_0$  increases if we choose

$$h_{n,k} = h_{n,k} + \epsilon \frac{\delta\Phi_0}{\delta h_{n,k}}, \quad (21)$$

with  $\epsilon$  a small step size, and similarly for  $\tau_{n,k}$  and  $\sigma_{n,k}$ .

We made use of a Matlab routine "minFuncBC", written by Mark Schmidt (<http://www.cs.ubc.ca/~schmidt/Software/minFunc.html>) to perform the final optimisation step (21). It makes use of a quasi-Newton method, the BFGS method, and accepted as input  $\Phi_0$  and the vector of derivatives with respect to the optimising parameters,  $\left[ \frac{\delta\Phi_0}{\delta h_{n,k}}, \frac{\delta\Phi_0}{\delta \tau_{n,k}}, \frac{\delta\Phi_0}{\delta \sigma_{n,k}} \right]$ .

#### IV. RESULTS

In order to optimise the pulses for as large a detuning space as possible, an initial single point in the detuning space was chosen by searching for the detuning point with optimised pulses that performed the best over the whole chosen detuning space. This entailed calculating the fidelity, using equation (14), for each point in the detuning space we would like to optimise, and then taking the average. Once the first point was found a second point would be chosen by searching for the second point that, together with the first, would result in the best optimised pulses. This process would be repeated until

$n$	1	2	3	4	5
$\tau_{n,k}$	$\tau_k$	$\tau_k - 0.15T_k$	$\tau_k + 0.15T_k$	$\tau_k - 0.4T_k$	$\tau_k + 0.4T_k$
$\sigma_{n,k}$	$\sqrt{0.2T_k}$	$\sqrt{0.2T_k}$	$\sqrt{0.2T_k}$	$\sqrt{0.25T_k}$	$\sqrt{0.25T_k}$
$n$	6	7	8	9	
$\tau_{n,k}$		$\tau_k - 0.55T_k$	$\tau_k + 0.55T_k$	$\tau_k - T_k$	$\tau_k + T_k$
$\sigma_{n,k}$		$\sqrt{0.2T_k}$	$\sqrt{0.2T_k}$	$\sqrt{0.32T_k}$	$\sqrt{0.32T_k}$

TABLE I: The parameters for each of the 9 gaussians that constitute each of the pulses. The amplitudes of the gaussians for a given pulse were all equal:  $h_{n,P} = h_{n,S} = 0.23\Omega_0$  and  $h_{n,St} = 0.23S_0$ .

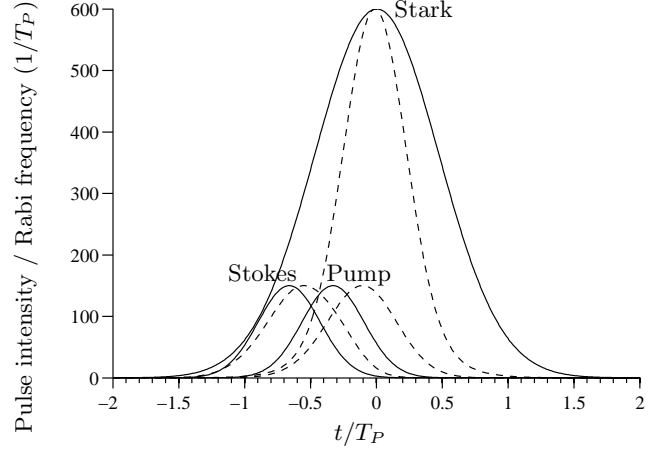


FIG. 3: The original gaussian pulses (solid lines) with  $S_0 = 200/T_P$ ,  $\Omega_0 = 50/T_P$ ,  $T_S = T_P$ ,  $T_{St} = 2T_P$ ,  $\tau_P = -T_P$ ,  $\tau_S = -2T_P$ . The dashed lines are the pulses optimised for the detunings shown in Figure 5.

no additional points result in better pulses. The total performance function used for evaluating the efficiency of the pulses during the optimisation on a number  $d$  of detunings was taken as the average of the performance functions (14) for each of the  $d$  detuning points,

$$\Phi = \frac{1}{d} \sum_x^d \Phi_0(\Delta_P^x, \Delta_S^x). \quad (22)$$

For the initial pulses used in our optimal control routine we used 9 gaussians of equal amplitude to approximate each of the original pulse shapes (2), (3) and (4). That is, in equation (13),  $q = 9$  and  $k \in \{P, S, St\}$  (the probe, Stokes and Stark fields). The parameters of these gaussians are given in Table I. The original pulses (solid lines in Figure 3) had the following parameters:  $S_0 = 200/T_P$ ,  $\Omega_0 = 50/T_P$ ,  $T_S = T_P$ ,  $T_{St} = 2T_P$ ,  $\tau_P = -T_P$ ,  $\tau_S = -2T_P$ ,  $\tau_{St} = 0$ .

The maximum of the optimised pulses was constrained to that of the original pulses ( $S_0 = 200/T_P$ ,  $\Omega_0 = 50/T_P$ ). If this is not done pulses can be made arbitrarily efficient by simply increasing the maximum Rabi

frequency. This is not physically possible due to adiabaticity constraints. Furthermore the optimisation was constrained to prevent the optimised pulses from becoming too narrow by setting the lower bound on the width of the pulses to 50% of the original pulse width. The optimised pulses are shown as the dashed lines in Figure 3.

The optimised pulses were then used to evaluate the fidelity of the population transfer from state  $|1\rangle$  to state  $|3\rangle$  for a range of detunings, keeping in mind that the chosen pulse ordering restricts the choice of detunings (10). As can be seen from Figures 4 and 5 the total “area” of detunings where population transfer is at all possible (the parts that are not black) is greatly increased when using the optimised pulses. The efficiency of the pulses can be gauged in a number of ways:

1. measuring the normalised “area” in detuning space where the pulses result in a fidelity greater than 0.8 for population transfer. For the original SCRAP pulses  $A_{>0.8}^{ori} = 0.131$ , whilst for the optimised pulses  $A_{>0.8}^{opt} = 0.178$  was obtained, an increase of 35.5%.
2. measuring the average fidelity over the whole detuning space, i.e. the sum of the fidelities for each point, divided by the number of points. For the original SCRAP pulses  $F_{av}^{ori} = 0.219$ , whilst for the optimised pulses  $F_{av}^{opt} = 0.321$ , an increase of 46.6%.
3. in Figure 6 a plot of the percentage increase for each point in the detuning space is presented. The  $\log_{10}$  of the percentage increase is used since some points had an initial fidelity of virtually zero and ended with a percentage increase of  $\approx 10^{23}\%$ .

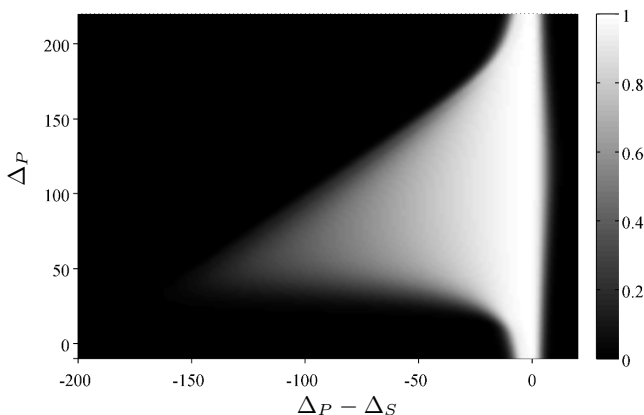


FIG. 4: The fidelity for a range of detunings, using the original gaussian pulses for SCRAP (shown as the solid lines in Figure 3), with  $S_0 = 200/T_P$ ,  $\Omega_0 = 50/T_P$ ,  $T_S = T_P$ ,  $T_{St} = 2T_P$ ,  $\tau_p = -T_P$ ,  $\tau_s = -2T_P$ . The decay out of state  $|2\rangle$  was  $\Gamma = 1/T_P$ .

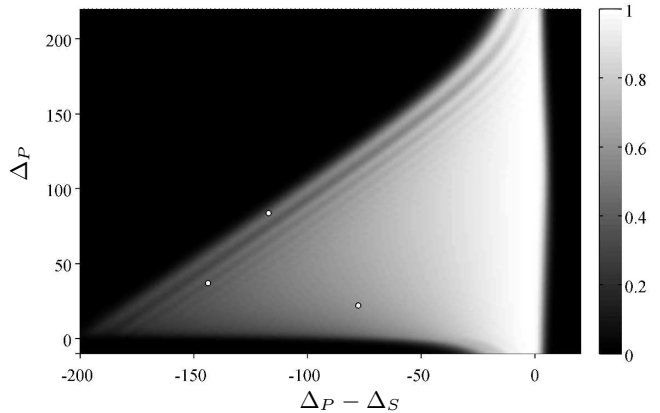


FIG. 5: The fidelity for a range of detunings, using SCRAP pulses optimised for the detunings indicated (white circles). Optimised pulses shown as the dashed lines in Figure 3. The decay out of state  $|2\rangle$  was  $\Gamma = 1/T_P$ .

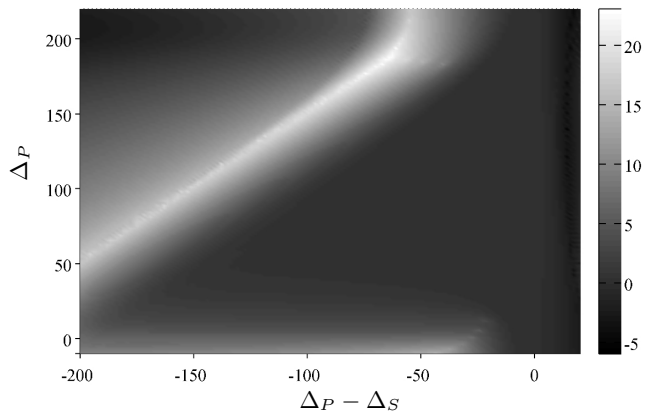


FIG. 6: The  $\log_{10}$  of the percentage increase in fidelity between standard SCRAP (Figure 4) and optimised SCRAP (Figure 5) for each point in the detuning space.

## V. CONCLUSIONS

It is clear that Stark-shift Chirped Rapid Adiabatic Passage (SCRAP) is a useful process to employ when trying to overcome inhomogeneous broadening of energy levels in a system undergoing state transfer. We have shown that the standard SCRAP pulses can be optimised so that a larger inhomogeneous broadening can be compensated for and so that the overall fidelity of state transfer for a range of detunings will be increased. Future work will aim to translate SCRAP into the quantum domain where the pump pulse is replaced by a quantum probe field carrying quantum information that is to be stored in the spin coherence of the atomic system.

### Acknowledgments

Johann-Heinrich Schönfeldt is supported by an MQRES scholarship from Macquarie University.

---

- [1] S. E. Harris, *Physics Today* **50**, 36 (1997).
- [2] L. V. Hau, S. E. Harris, Z. Dutton, and C. H. Behroozi, *Nature* **397**, 594 (1999).
- [3] D. F. Phillips, A. Fleischhauer, A. Mair, R. L. Walsworth, and M. D. Lukin, *Phys. Rev. Lett.* **86**, 783 (2001).
- [4] M. Fleischhauer and M. D. Lukin, *Phys. Rev. A* **65**, 022314 (2002).
- [5] M. D. Lukin, *Rev. Mod. Phys.* **75**, 457 (2003).
- [6] J.-H. Wu, G. C. L. Rocca, and M. Artoni, *Phys. Rev. B* **77**, 113106 (2008).
- [7] A. V. Turukhin, V. S. Sudarshanam, M. S. Shahriar, J. A. Musser, B. S. Ham, and P. R. Hemmer, *Phys. Rev. Lett.* **88**, 023602 (2001).
- [8] J. J. Longdell, E. Fraval, M. J. Sellars, and N. B. Manson, *Phys. Rev. Lett.* **95**, 063601 (2005).
- [9] C. Wei and N. B. Manson, *Journal of Optics B: Quantum and Semiclassical Optics* **1**, 464 (1999).
- [10] P. R. Hemmer, A. V. Turukhin, M. S. Shahriar, and J. A. Musser, *Opt. Lett.* **26**, 361 (2001).
- [11] A. A. Rangelov, N. V. Vitanov, L. P. Yatsenko, B. W. Shore, T. Halfmann, and K. Bergmann, *Phys. Rev. A* **72**, 053403 (2005).
- [12] N. Khaneja, T. Reiss, C. Kehlet, T. Schulte-Herbrüggen, and S. J. Glaser, *J. Magn. Reson.* **172**, 296 (2005).
- [13] L. P. Yatsenko, B. W. Shore, T. Halfmann, K. Bergmann, and A. Vardi, *Phys. Rev. A* **60**, R4237 (1999).
- [14] T. Rickes, L. P. Yatsenko, S. Steuerwald, T. Halfmann, B. W. Shore, N. V. Vitanov, and K. Bergmann, *J. Chem. Phys.* **113**, 534 (2000).